Development 129, 3255-3267 (2002)
Printed in Great Britain © The Company of Biologists Limited 2002
DEV8925

daughterless coordinates somatic cell proliferation, differentiation and germline cyst survival during follicle formation in *Drosophila*

John E. Smith III, Craig A. Cummings† and Claire Cronmiller*

Department of Biology, University of Virginia, P.O. Box 400328, Charlottesville, VA 22904-4328, USA
†Present address: Department of Microbiology and Immunology, Stanford University, Stanford, CA 94305, USA
*Author for correspondence (e-mail: crc2s@virginia.edu)

Accepted 12 April 2002

SUMMARY

During *Drosophila* oogenesis two distinct stem cell populations produce either germline cysts or the somatic cells that surround each cyst and separate each formed follicle. From analyzing *daughterless (da)* loss-of-function, overexpression and genetic interaction phenotypes, we have identified several specific requirements for da^+ in somatic cells during follicle formation. First, *da* is a critical regulator of somatic cell proliferation. Also, *da* is required for the complete differentiation of polar and stalk cells, and elevated *da* levels can even drive the convergence and extension that is characteristic of interfollicular stalks. Finally, *da* is a genetic regulator of an early checkpoint for germline cyst progression: Loss of *da* function inhibits normally occurring apoptosis of germline cysts at the region 2a/2b boundary of the germarium, while *da* overexpression leads to postmitotic cyst degradation. Collectively, these *da* functions govern the abundance and diversity of somatic cells as they coordinate with germline cysts to form functional follicles.

Key words: Oogenesis, *daughterless*, bHLH, E protein, *Drosophila melanogaster*

INTRODUCTION

A fundamental question in developmental biology is how broadly expressed multifunctional regulators can effect diverse and specific morphogenetic events throughout development. A good example of such a regulator is the *daughterless* gene product in *Drosophila*. Da is an E protein, or Class 1 helix-loop-helix (HLH) transcription factor (Murre et al., 1994), which heterodimerizes with various Class 2 HLH proteins to form transcriptional activation complexes involved in many developmental processes, including sex determination, neurogenesis, myogenesis, and oogenesis (Caudy et al., 1988; Cummings and Cronmiller, 1994; Deshpande et al., 1995; Gonzalez-Crespo and Levine, 1993; Keyes et al., 1992). In some specific cases the mechanisms of *da* function have been elaborated, such that Da binding partners and/or targets have been identified. For example, during sex determination Da heterodimerizes with Scute (Sc/Sis-b) to activate *Sxl* transcription in females, and during neurogenesis Da pairs with Sc or Achaete (Ac) in subsets of cells to promote neural differentiation (Cabrera and Alonso, 1991; Yang et al., 2001). In other cases *da* is known to be required for the expression of specific genes in fully differentiated cell types (King-Jones et al., 1999; Misquitta and Paterson, 1999). For most of *da*'s developmental roles, however, the specific regulated processes have not been detailed.

Several lines of evidence suggest that a general role of *da* is to regulate proliferation and cell cycle progression. In *da* mutant embryos transcription of several cell cycle genes is reduced or eliminated in the peripheral nervous system precursors (Hassan and Vaessin, 1997). In larval eye discs, *da* mutant clones in the posterior region of the morphogenetic furrow do not accumulate cyclin B, indicating that the cell cycle is blocked in G_1 (Brown et al., 1996). In the larval optic lobes overexpression of the Class 2 HLH *asense (ase)*, a Da binding partner (Jarman et al., 1993), results in reduced mitotic activity, while loss of function causes an increase in mitotic activity (Wallace et al., 2000). Overexpression of *da* in embryonic mesodermal tissue culture cells drives *nautilus*-dependent cell cycle arrest and concomitant differentiation into muscle (Wei et al., 2000). Finally, numerous observations that the Da-related E proteins in mammals affect cell proliferation and/or cell cycle progression (Pagliuca et al., 2000; Peverali et al., 1994; Zhao et al., 2001) suggest that cell cycle control may be an inherent functional activity of this evolutionarily conserved protein family, of which Da is the only member in *Drosophila*.

One morphogenetic process for which *da* function is critical is ovarian follicle formation, which requires the coordinated control of the proliferation and differentiation of both germline and somatic cells. Stem cells for both the germline and soma reside in the germarium, at the anterior end of each ovariole of the ovary (see Fig. 1A). At the anterior of the germarium, overlying somatic cells create a niche to maintain the germline stem cells (Spradling et al., 2001; Xie and Spradling, 2000). One of the two germline stem cells undergoes an asymmetric division to produce another stem cell and a cystoblast. The cystoblast undergoes four rounds of mitotic division with

incomplete cytokinesis to produce a germline cyst, containing one oocyte and fifteen interconnected nurse cells, within region 2a of the germarium. Morphologically unidentifiable somatic stem cells reside in region 2 of the germarium and give rise to mesenchymal somatic cells that surround each germline cyst and compress it into the characteristic lens shape of region 2b of the germarium. As the somatic cells continue to envelop the cyst, they differentiate into an epithelial monolayer to form a follicle. Each follicle is separated from the previously (and subsequently) formed follicle by additional somatic cells, which form a stalk. In *da* loss-of-function mutants, phenotypes include absence of interfollicular stalks, compound follicles in which two cysts are incompletely separated by somatic cells, bicyst follicles in which two cysts are neatly packaged inside an epithelial monolayer, and more extreme compound follicles in which multiple cysts are improperly packaged and can include the contents of an entire ovariole (Cummings and Cronmiller, 1994). The consequence of all of these defects is loss of egg production, and this sterility can be traced conceptually back to defects in the morphogenetic sequence that leads to follicle formation in the germarium.

In this paper we identify specific morphogenetic events that are regulated by *da* during oogenesis. From analyzing both *da* loss-of-function and overexpression phenotypes, as well as genetic interactions, we demonstrate a role for *da* in somatic cell proliferation. We also show that *da* is required for complete differentiation of stalk and polar cells. Finally, we document a somatic requirement for *da* for the germline cyst apoptosis that is a component of the cyst progression checkpoint in the germarium that has been previously described (Drummond-Barbosa and Spradling, 2001).

MATERIALS AND METHODS

Drosophila stocks and genetics

Flies were raised on either a yeast-agar-dextrose or molasses-cornmeal-yeast medium (details available on-line: http://dev.biologists.org/supplemental/) at approximately 25°C. The wild-type strain used was OregonR; other stocks are listed in Table 1.

Table 1. Fly stocks used in this study

Stock*	Source
***da* alleles**	
cl da^2/CyO	
cn da^{lyh}/CyO	
cl da^{s22}/CyO	
cl da^7 b pr cn/CyO	
Dp(2;2)da^+20	
Dp(2;Y)B231	
Enhancer traps	
A101/TM6	P. Adler
y w; B1-93F	H. Ruohola-Baker
cn; l(3)01344/TM3, ry^{RK} Sb	A. Spradling
Transgenic lines	
w; P(w^+, hsp70-da^+)	A. Singson
hs-hhM11	H. Lin
Used in genetic interactions	
Su(H)/In(2L)Cy, In(2R)Cy	Bloomington†
dx^{S1M} t^2 v/FM6	I. Dawson
ec dx^1	Bloomington
ed Su(dx)^2	Bloomington
hop^2/FM7a	Bloomington
Stat92E^{1681}/TM3	C. Dearolf
grk^{HK36} cn bw/CyO	T. Schüpbach
grk^{WG41} cn bw sp/CyO	T. Schüpbach
spi^{A14}/CyO	N. Perrimon
spi^{OE92}/CyO	N. Perrimon
top^{IP02} cn bw sp/CyO	J. Price
top^1 bw/CyO	J. Price
sev^{d2}; drk^{eOA}/CyO	G. Rubin
sev^{d2}; sos^{e4G}/CyO; ry	G. Rubin
sev^{d2}; Ras85D^{e1B}/TM3	G. Rubin
w phl^7 P{FRT(w[hs])}101/FM7	N. Perrimon
Dsor1^{S-1221}/DPY3610/C(1)yw	G. Rubin
rl^{S-135}/CR2 (CyO, sev-Ras1UR)	G. Rubin
phl^{C110}; b rl^{Sem}/+	E. Hafen
pnt^{7825}/TM3, Sb	G. Rubin
aop^{IP}/CyO	S. DiNardo
aop^{IIS}/CyO	S. DiNardo
w brn$^{fs.107}$/FM3	A. Mahowald
y w brn$^{1.6P6}$/FM7a	A. Mahowald
sev^{d2}	G. Rubin
h boss; ry	G. Rubin

*Additional information on alleles is available at http://flybase.bio.indiana.edu/ (FlyBase, 2002).
†Bloomington Stock Center.

Heat shock treatments

da overexpression

Flies carrying four copies of the p_{hsp70}-da^+ transgene in an otherwise wild-type background were given a pulse of 30 minutes at 37°C four times per day for 6 days. Flies carrying two copies of the p_{hsp70}-da^+ transgene in the da^{lyh} mutant background were reared at 25°C and shifted to 32°C for 6 days.

ectopic *hh* expression

Flies carrying one copy of the p_{hsp70}-hh^+ transgene received pulses of 1 hour at 37°C twice daily for 5-6 days; the regime began 24-48 hours after eclosion.

Staining

Ovaries were fixed and DAPI stained as previously described (Cummings and Cronmiller, 1994). Enhancer trap lines were stained using X-gal substrate or immunostained using anti-β-galactosidase (1:10,000; Cappel) as previously described (Cummings and Cronmiller, 1994). Monoclonal mouse anti-FasIII 2D5 (1:10) (Patel et al., 1987), monoclonal mouse anti-Hts 1B1 (1:10, Developmental Studies Hybridoma Bank) (Zaccai and Lipshitz, 1996) and polyclonal rabbit anti-Vasa (1:1000) (Styhler et al., 1998) were detected using FITC- or TRITC-conjugated secondary antibodies (1:300, Jackson Immunoresearch).

Acridine Orange

Acridine Orange is a vital stain for apoptotic nuclei, which are visible with a filter for green fluoresence, and for lysosomes that associate with fragmenting nuclei, which are visible with a filter for red fluorescence (Mpoke and Wolfe, 1997). Ovaries were dissected in Shields and Sang M3 insect medium (Sigma), stained for 15 minutes in Acridine Orange (5 μg/ml in M3 medium), and washed for 15 minutes in M3 medium. Similar results were obtained using PBS; germarium staining was dose- and site-dependent, with considerably lower intensity in the germarium compared to apoptotic stage 13 nurse cells or occasional stage 8 apoptotic follicles in which the follicle maturation checkpoint had been activated. A dramatic enhancement of the germarial staining was observed when samples were dissected in PBS, stained with Acridine Orange (5 μg/ml) or Nile Blue A (100 μg/ml) in hypotonic 0.1 M sodium phosphate buffer, pH 7.2, and washed 15 minutes in PBS [based on Abrams et al. (Abrams et al., 1993)]. For our standard Acridine Orange staining protocol (Fig. 5D

and supplemental data: http://dev.biologists.org/supplemental/), ovaries were dissected from flies reared on molasses-cornmeal-yeast medium at 25°C, placed in Acridine Orange (5 μg/ml in 0.1 M sodium phosphate buffer, pH 7.2) for 1-2 minutes, transferred to PBS on a slide and immediately scored.

TUNEL

TUNEL reagents (Roche Molecular Biochemicals) were used as an independent means of detection of apoptotic cells, since TUNEL preferentially labels apoptotic cells relatively late in the apoptotic process (Barrett et al., 2001; Gold et al., 1994). Ovaries were dissected in PBS, fixed in 4% paraformaldehyde (in PBS), and processed according to manufacturer's protocol.

Image processing

All images were either captured on film or with a MagnaFire Camera (Optronics) on a Zeiss (Axiophot/Axioskop) microscope. Captured images were processed and annotated in Adobe Photoshop. Images depict FITC as green and TRITC as magenta (overlap white) to make the images color-blind-accessible.

RESULTS

da is required for somatic cell proliferation

To identify specific cellular processes that are regulated by *daughterless* in the ovary, we examined the complete loss-of-function phenotype using the ovary-specific null allele da^{lyh} (Smith and Cronmiller, 2001). Mutant ovaries were stained with antibodies against Vasa, a germline-specific marker, and Hts, a marker for the somatic cytoskeleton and the specialized germline organelles, the spectrosome and fusome.

At eclosion every *da* ovariole was already defective (Fig. 1C-E, compare to 1B). Normal follicles were generally not observed, except in an occasional ovariole that contained at most a single properly formed follicle. By examining ovaries at eclosion and noting the presence of the basal stalk on each ovariole, we were able to ensure that we scored the phenotype of every germline cyst produced within an ovariole. Each follicle attached to a basal stalk contained a single germline cyst, the first generated in that ovariole. In 90% of the ovarioles, the second and third germline cysts produced were likewise individualized into follicles; however, follicles in these ovarioles were never separated by interfollicular stalks (Fig. 1C,D). Follicles containing the first germline cyst produced were generally complete, namely the cyst was surrounded by a continuous epithelium, as indicated by the presence of two discrete epithelial layers between the first and second cysts. Such a double epithelial layer was less commonly observed between the second and third cysts, which instead appeared to share a disorganized layer of somatic cells that more closely resembled undifferentiated mesenchymal cells than differentiated epithelial cells. Similarly appearing cells also separated the next youngest cysts in the ovariole, which would correspond to the germarium/vitellarium junction in wild type. In the remaining 10% of the ovarioles, the first germline cyst was contained in a properly formed follicle that was separated from the next youngest cyst and its follicular epithelium by an interfollicular stalk: these were the only completely normal follicles observed (Fig. 1E). Invariably, in such ovarioles, the second and third cysts were contained within a single continuous epithelium. These bicyst follicles appeared to have arisen because there were insufficient somatic

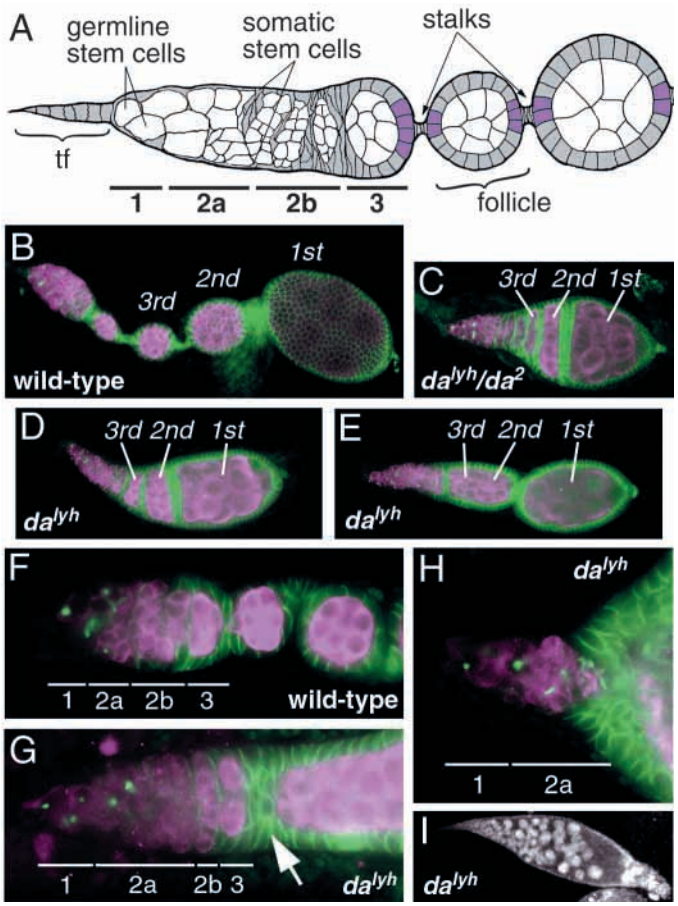

Fig. 1. The *da* loss-of-function phenotype. (A) Diagram of the anterior end of an ovariole, including terminal filament (tf), subdivided germarium (with regions indicated), and early follicles of the vitellarium. Somatic cells (gray), polar cells (purple) and stalks are indicated. Wild-type (B,F), da^{lyh}/da^{2} (C), da^{lyh}/da^{lyh} (D,E,G,H) ovaries were costained for Hts (Hu li tai shao; green) and Vasa (magenta). At eclosion most *da* null ovarioles (C,D) have no distinct interfollicular stalks; in 10% of ovarioles (E), the posteriormost follicle is separated by a stalk, but always at the expense of the follicular epithelium of the second germline cyst produced. (G) Older *da* mutant ovaries, despite extensive defects within the vitellarium, have typical germarium morphology. Interfollicular stalks do not form, even when sufficient somatic cells accumulate (arrow) adjacent to follicles with multiple cysts. (H) In more extreme examples, regions 2b and 3 are lost within the compound follicles that constitute the remainder of the ovariole. (I) A typical DAPI-stained da^{lyh} ovariole. Images B-E are at the same scale, as are images F-H.

cells to surround the second germline cyst. This suggests that the number of available somatic cells located between the first and second cysts was sufficient to contribute to an interfollicular stalk in this position only at the expense of the epithelium of the second cyst. Finally, the frequency of completely normal follicles is consistent with the fecundity of da^{lyh} females, each of which can lay up to 5 eggs before completely ceasing oviposition; thus, follicles not separated by stalks never give rise to functional eggs.

In maturing females, although the *da* mutant phenotype is so severe that follicular structure is almost completely disrupted (Cummings and Cronmiller, 1994; Smith and

Cronmiller, 2001), we found that the overall organization of the germarium appeared to be undisturbed. Based on the appearance of spectrosomes, fusomes and germline cysts, all four regions of the germarium generally could be distinguished in da^{lyh} mutants, and their arrangement was indistinguishable from wild type (Fig. 1F,G). In da^{lyh} germaria, however, there was an increased distance between regions 1 and 2b relative to wild type, suggesting the presence of an increased number of germline cysts in region 2a (Fig. 1G). Also, in region 3 of the germarium, where somatic cells normally differentiate into an epithelial monolayer to envelop each germline cyst, there was no evidence of constriction by somatic cells in the posterior region to complete follicle individualization. This could be due to insufficient somatic cells to form the necessary interfollicular stalk, consistent with our observations of ovaries from newly eclosed females. However, even in germaria that were connected to multicyst follicles, where the somatic cell number was greater than in wild type (arrow, Fig. 1G), stalks still failed to form. Thus, the absence of a distinct junction between the germarium and vitellarium in *da* mutant ovaries results not only from defective cell number but also from aberrant cell behavior. In the extreme, as mutant defects accumulated with age, even previously organized regions of the germarium were lost, as regions 2b and 3 were no longer distinguishable (Fig. 1H).

da regulates differentiation

Because aberrant somatic cell behavior appeared to contribute to the *da* mutant phenotype, we examined the expression of cell markers to determine whether specific cell types were affected. For interfollicular stalk cells, we examined two markers, *B1-93F* (Fig. 2A) and *l(3)01344* (Ruohola et al., 1991; Forbes et al., 1996a). Even though stalks were not evident in *da* mutant ovaries, cells expressing stalk cell markers were still present. *B1-93F*-expressing cells formed either small clumps on the edge of a junction of two follicles that were not separated by a stalk (data not shown) or small clusters or rope-like strings of cells within the epithelium in conjunction with more extreme phenotypes (Fig. 2B,C). Expression of the stalk cell marker was drastically reduced in both the strong hypomorphic and null mutant genotypes, such that staining was consistently detectable only with two copies of the enhancer trap reporter. Identical observations were made with *l(3)01344* (data not shown). So, *da* may be a transcriptional regulator of the genes identified by both of these enhancer traps; however, this regulation would have to be cell specific, since enhancer trap expression in the terminal filament was not affected (Fig. 2C). Alternatively, *da* may be required for complete differentiation of stalk cells, resulting in an indirect effect upon enhancer trap expression, which is only one characteristic of the differentiated state.

For polar cells we also examined two markers, the *neuralized* enhancer trap *A101* and FasIII protein. Generally, *A101* marks a pair of polar cells at both the anterior and posterior ends of each follicle (Johnson et al., 1995), although initial expression at the beginning of the vitellarium often encompasses polar clusters of up to 4 cells (Fig. 2D). In moderately severe *da* mutant ovaries, *A101* was expressed in clusters of 3 or 4 cells in positions that corresponded to the poles of germline cysts (Fig. 2E). In severely disrupted ovarioles, larger numbers of *A101*-positive cells seemed to accumulate in a section of the ovariole anterior to the gross degeneration that is typical of the extreme *da* phenotype (Fig. 2F). Unlike *A101*, FasIII is initially expressed at high levels in all somatic cells in region 3 of the germarium; the expression pattern gradually refines to resemble that of the *A101* marker (Fig. 2G). The pattern of FasIII-staining-cells in *da* mutants was similar to that of *A101*, namely clusters of 2-4 strongly staining cells at the polar boundaries of cysts (Fig. 2H,I). Both polar cell markers indicate that there is no loss of this class of

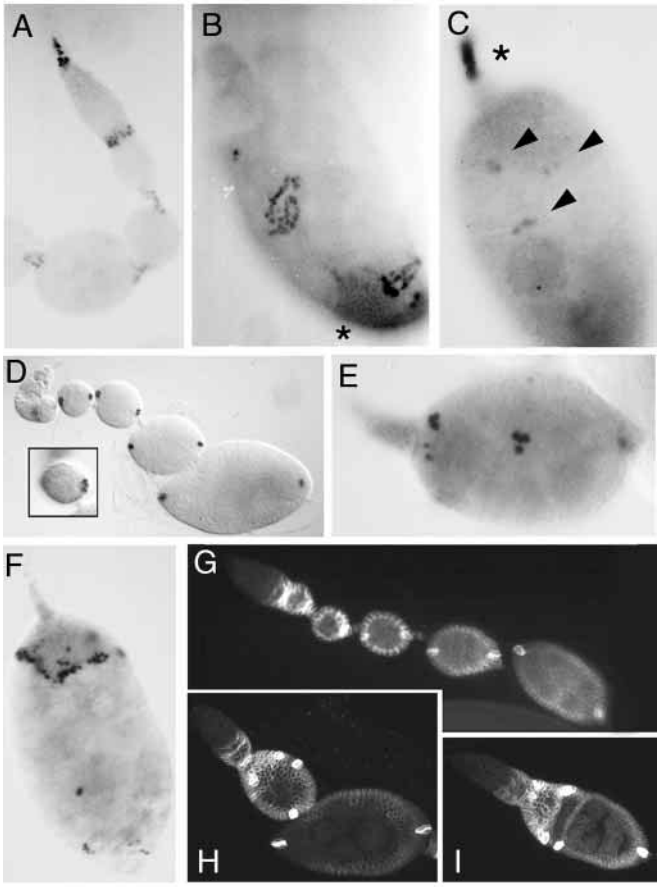

Fig. 2. The effect of *da* on polar and stalk cell markers. (A) Enhancer trap *B1-93F* marks interfollicular stalks, presumptive stalk cells and terminal filament in wild type. In da^{7}/da^{s22} (B) and da^{lyh} (C) ovaries the enhancer trap stains clusters of cells that are sometimes arranged into rope-like patterns. Expression of *B1-93F* is weaker in *da* mutants (C, arrowheads) relative to the overexposed terminal filament (C, asterisk). This enhancer trap is also expressed in degrading somatic cells often present at the posterior of *da* mutant ovarioles (B, asterisk). (D) In wild type, enhancer trap *A101* stains polar cells in each follicle; initial expression may include up to 4 cells at either pole (3 shown in inset), but by stage 4 staining is limited to 2 cells at each pole. (E) In da^{7}/da^{s22} mutant ovaries, clusters of 3 or 4 somatic cells are found throughout ovarioles, apparently corresponding to ends of each cyst in a compound follicle. (F) In more severely disrupted *da* mutant ovarioles, a large number of *A101*-positive cells are found throughout a region that is anterior to extensive degradation. (G) In wild type, FasIII protein is found initially in all somatic cells in regions 2b and 3 of the germarium; levels subsequently diminish in all but the polar cells. (H-I) In *da* mutants, clusters of 3 or 4 FasIII-positive cells are found along compound follicles, corresponding to cyst poles.

somatic cells in *da* mutants; in fact, mutant polar cell clusters included one or two extra cells. One possible explanation for the extra cells is that *da* is required for the narrowing of polar cell number that normally accompanies polar cell differentiation. Alternatively, if *da* is required for timely terminal differentiation of polar cells, then one extra cell division in the mutant would account for the increased polar cell cluster size.

Effects of increased Da levels

The consequences of increased *da* dose on follicle formation also demonstrated a role for *da* in somatic cell proliferation. Ovaries from flies that carry an extra copy of da^+ in a tandem duplication (*Dp20*) have normal ovariole morphology, but the interfollicular stalks are longer (Fig. 3B, compare with 3A) (Smith and Cronmiller, 2001). In flies that carried an extra copy of da^+ in a chromosomal transposition (*DpB231*), in addition to longer stalks we observed an increased number of previtellogenic follicles (Fig. 3C-E). The average number of stage 2-7 follicles per ovariole was significantly higher in *DpB231* ovaries relative to wild type: 5.4±0.07 (s.e.m.) versus 4.8±0.04 (P<0.01, *t*-test). Thus, the rate of follicle production in *DpB231* was higher than in wild type. The increases in stalk length and rate of follicle formation indicate that excess da^+ leads not only to increased somatic cell proliferation, but also to either increased germline cyst production or reduced germline cyst loss at the region 2a/2b checkpoint. The additional ovarian phenotype of *DpB231* can be accounted for by the higher level of da^+ function it provides relative to *Dp20*; this was corroborated by the strength of their genetic interactions with da^{lyh} (data not shown).

Using additional genetic tools, we were able to generate flies with even higher levels of da^+, and we found that greater overexpression led to aberrant somatic cell behavior. These higher levels were obtained by combinations of heat-inducible da^+ transgenes, *DpB231* and da^{lyh}, which upon transactivation produces higher than wild-type levels of da^+ function (Smith and Cronmiller, 2001). Sustained elevated da^+ levels resulted in the occurrence of what appeared to be ectopic stalks that formed at the expense of follicular epithelium; these stalks were stretched superficially along germline cysts that were incompletely enveloped by a somatic epithelium (Fig. 4A,B). We never saw an incompletely enveloped germline cyst without an ectopic stalk associated with it, and conversely we never saw an ectopic stalk unless it was in direct contact with a germline cyst that lacked substantial somatic epithelium. Thus, elevated Da protein was capable of driving stalk cell differentiation. Even intermittent da^+ overexpression led to follicular defects: pulsatile induction of p_{hsp70}-da^+ transgenes resulted in an elongation of the germarium (Fig. 4D,E). Several morphological flaws contributed to the protracted appearance of these germaria: failure of cysts in region 2b to compress into their characteristic lens shape, retention of intact older follicles that never individualized, and narrowed and elongated posterior regions. All of these flaws likely resulted from aberrant somatic cell behavior and may indicate defects in differentiation. Cells anterior to unbudded follicles (asterisks, Fig. 4D,E) failed to differentiate into stalks. The Da-overexpressing somatic cells throughout regions 2b and 3 and surrounding the attached follicles appeared to squeeze the underlying germline cysts.

Elevated Da levels also produced germline defects in older females. As we previously reported, Da overexpression can lead to germaria that attach directly to mid-to-late stage follicles (Smith and Cronmiller, 2001). In the overexpression genotype, *DpB231;*da^{lyh}, every germarium showed loss of region 2b and 3 cysts by two weeks of age (arrow, Fig. 4F). Loss of cysts could result from a cessation of both cyst production and posterior progression or from the degradation of cysts. The latter appeared to be the case here, since dying cysts (identified by decreased Vasa staining) were found in the posterior of the germarium (arrows, Fig. 4F,G) and in newly formed follicles (arrow, Fig. 4H). Occasionally, faint Vasa staining was found within long stalks, indicating the presence of cyst remnants just prior to their complete degradation (arrow, Fig. 4I). In the germarium, degradation and loss of germline cysts permitted the spread of mitotically active cysts, normally confined to region 2a, to more posterior regions of the germarium (Fig. 4G,H). Consequently, cysts that were still dividing slipped to the posterior end of the germarium, resulting in their premature envelopment by somatic cells (arrowhead, Fig. 4J). Similarly, at the anterior end stem cells occasionally slipped out of the germline niche completely and were lost, as evidenced by the lack of any characteristically round spectrosomes at the very anterior of the germarium (arrowhead, Fig. 4K). In rare cases the germline component was completely lost from the germarium (Fig. 4L). Thus, elevated Da levels resulted in degradation of post-mitotic germline cysts and led indirectly to loss of germline stem cells.

da loss-of-function mutants suppress normal germline apoptosis in the germarium

In *da* loss-of-function mutants we found the converse relationship between *da* function and germline viability, namely, reduced *da* protected germline cysts from degradation. Although cyst degradation has not been reported in wild-type germaria [except under nutrient-deprived conditions (Drummond-Barbosa and Spradling, 2001)], we observed apoptosing cysts in region 2a/2b of wild-type germaria (from flies reared on either of two nutrient-rich media) when we assayed cell death by two different methods, vital staining (Acridine Orange and Nile Blue) and TUNEL. Acridine Orange staining was detected with filters for green fluorescence, where apoptotic cells were visible as bright spots against diffuse background staining (Fig. 5A); however, staining was most dramatic with filters for red fluorescence, where the highest concentrations of Acridine Orange fluoresced with no general background staining (Fig. 5A′). Localized within region 2 of the germarium, the largest bright spots could often be correlated with blebs on the germarium surface that were visible under DIC or phase contrast (data not shown). At a low frequency, smaller punctate fluorescence was was observed as an outline of the germarium, apparently restricted to the space between the germarium and the overlying epithelial sheath; this distinct acellular background staining did not reflect apoptosis, since it was never observed following TUNEL. Because apoptosis in wild-type germaria was unexpected, we repeated the vital stain analyses numerous times, varying the dissection and staining solutions (phosphate buffer, PBS, M3 insect medium), and in spite of minor trial-to-trial variation, Acridine Orange fluorescence in region 2 of the germarium was always observed. Establishing a standard

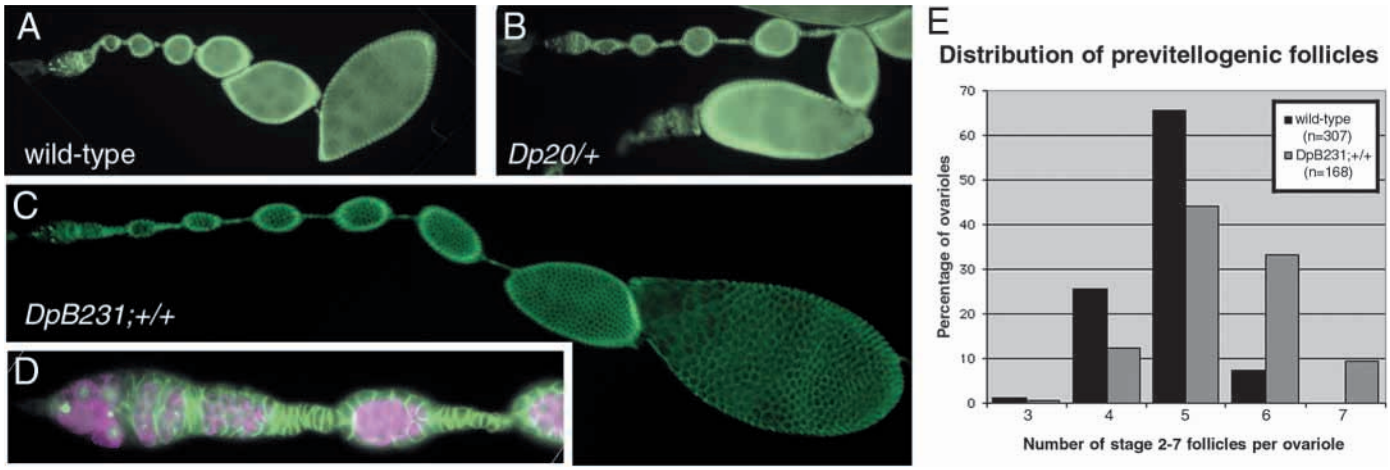

Fig. 3. Chromosomal da^+ duplications produce excess somatic cells. Ovaries from *3X-da*$^+$ flies (B, C) have longer interfollicular stalks than wild-type ovaries (A). (D) Enlargement of the anterior end of ovariole shown in C. (E) Ovaries with the B231 duplication (which includes da^+) also produce more follicles than wild type, as indicated by the number of previtellogenic follicles per ovariole and (C) increased ovariole length. Staining: Hts (green), Vasa (magenta).

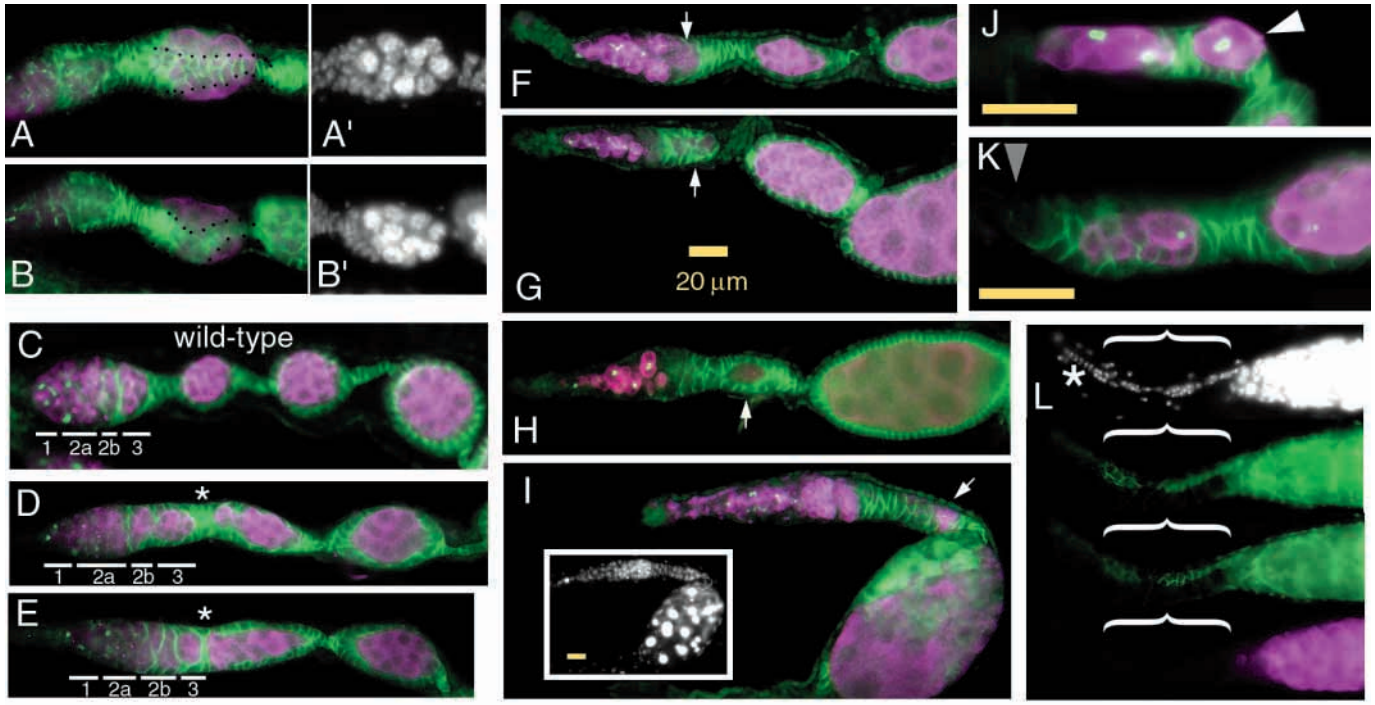

Fig. 4. Elevated da^+ levels were achieved with several genotypes and environmental conditions: (A,B) homozygous da^{lyh} with p_{hsp70}-da^+, 6 days at 32°C; (D,E) p_{hsp70}-da^+, 37°C pulses; (F-L) homozygous da^{lyh} with *DpB231*. (A,B) High levels of da^+ drive formation of ectopic stalks at the expense of epithelium; partially exposed germline cysts (A′,B′) have stalk-like somatic cells (demarcated with black dots in A, B) that stretch along the cyst. (D,E) Pulses of Da result in aberrant somatic behavior; new cysts are elongated and initially fail to separate from the germarium (asterisks, compare to wild type, C). (F-L) Elevated *da* levels result in germline cyst degradation. Cyst remnants with decreased Vasa are seen in regions 2b and 3 of the germarium (arrows, F,G), in newly formed follicles (arrow, H) and in long stalks (arrow, I). Degrading compound follicles, with extensive Vasa staining (I,L‴) are identifiable by DAPI (inset I,L). (H-J) In germaria depleted of mature cysts, still-dividing germline cysts, normally confined to region 2a, spread posteriorly and become surrounded by somatic cells. A late interphase 4-cell cyst (arrowhead, J) in region 3 is identifiable by its fusome structure (de Cuevas and Spradling, 1998) and DAPI (data not shown). (K) Spreading germline cells occasionally fall out of the germline stem cell niche (gray arrowhead points to empty niche). (L-L‴) DAPI staining (L) and (L′-L‴) different focal planes through a germlineless germarium. Germarium (bracket) without any germline (L‴) is identifiable by the terminal filament (asterisk in L). Staining: DAPI (grayscale), Hts (green), Vasa (magenta). Yellow scale bar: 20 μm; all images same magnification as G except I, J and K.

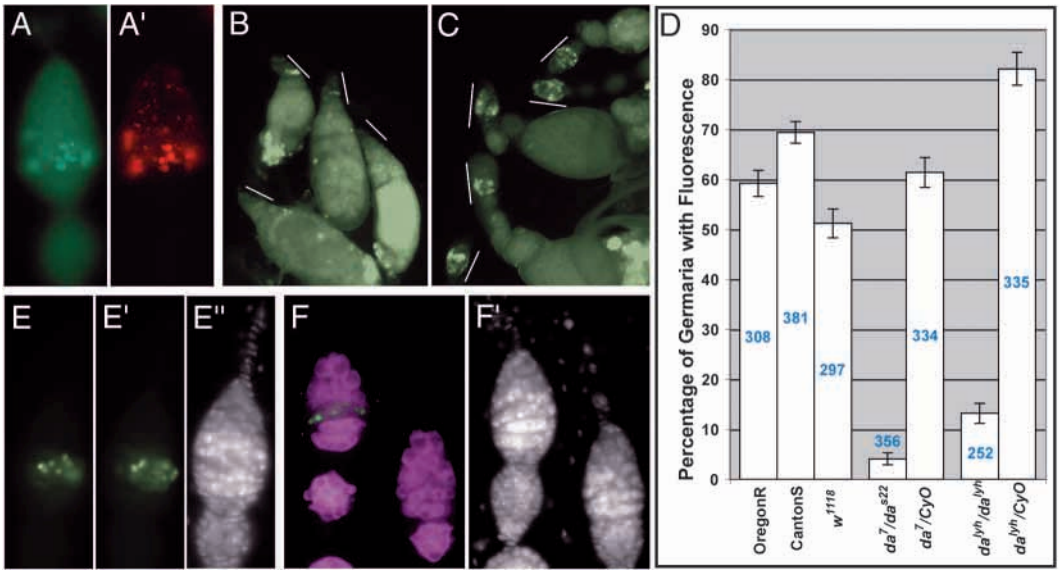

Fig. 5. Visualization of the cyst progression checkpoint. Acridine Orange staining (A,A′,B,C) and TUNEL (E,E′,F) identify apoptotic germline cells in region 2 of the germarium. Vital Acridine Orange staining of wild-type germaria in M3 medium is visible as green (A) or red (A′) fluorescence; signal is localized to region 2 of the germarium. (B-C) In phosphate buffer, where Acridine Orange signal is amplified, da^{lyh} mutants (B) show dramatically reduced fluorescence relative to wild type (C). (B,C are shown at the same magnification; lines indicate the positions of the germaria for comparison.) (D) Apoptosis as measured by vital Acridine Orange staining of germaria from 2- to 4-day old adult wild-type and *da* mutant females. Blue numbers indicate total number of germaria scored; bars show the average percentage per female ±s.e.m. (n=11 for da^{7}/da^{s22}, n=10 for all others). (E,E′) TUNEL (green) labels cells at the region 2a/2b boundary; staining corresponds with decreased DAPI intensity (E″). (F,F′) Reduced Vasa (magenta) identifies apoptotic cells as germline and corresponds with smaller punctate DAPI staining.

staining protocol, we quantified the frequency of apoptosis in wild-type germaria of typical laboratory strains (OregonR, CantonS, and the commonly used transformation host $white^{1118}$) (Fig. 5D and supplemental data: http://dev.biologists.org/supplemental/). Each strain had a high frequency of Acridine Orange staining in the germaria, yet the specific frequency varied with each genotype. Additionally, the frequency increased with age, e.g. in OregonR females the frequency of Acridine Orange-staining germaria increased to over 90% (supplemental and unpublished data). Evidence of apoptosis was even more dramatic from TUNEL assays, which were routinely more consistent than the vital staining methods and allowed costaining for Vasa and DNA (DAPI). TUNEL-positive cells were restricted to the region 2a/2b boundary, often transecting the germarium and indicating the apoptosis of the entire interconnected cyst (Fig. 5E,E′). As with Acridine Orange, TUNEL-positive cells often corresponded to blebs on the germarium surface (data not shown); the label also often coincided with either reduced DAPI intensity (Fig. 5E″) or bright punctate DAPI staining (Fig. 5F′). Colocalization of Vasa protein with TUNEL indicated that the apoptotic cells were germline in origin (Fig. 5F), and the level of Vasa in these degrading cells was markedly lower than in the neighboring viable cysts, reminiscent of the reduced Vasa seen in degrading cysts of *da*-overexpressing ovaries (Fig. 4F). In contrast to wild type, *da* loss-of-function mutant germaria rarely contained apoptotic cells, when assayed by either vital staining or TUNEL. Various mutant genotypes (da^{lyh}, $da^{lyh}/Df(da)$ and da^{7}/da^{s22}) consistently showed a drastic reduction or complete absence of Acridine Orange and Nile Blue staining in the germarium under various conditions (Fig. 5B-D and data not shown). Again using our standard Acridine Orange staining protocol, we quantified the frequency of apoptosis in germaria of *da* mutant females and their heterozygous siblings, thus controlling for genetic background effects. Both da^{7}/da^{s22} and da^{lyh} ovaries showed a dramatic reduction in Acridine Orange staining relative to both the wild-type strains and the sibling controls (Fig. 5D). In *da* mutants, the effect of age on the frequency of Acridine Orange staining could not be assayed, since flies older than 2-4 days had extensive degradation within the ovarioles that precluded scoring in the germarium. In germaria of da^{lyh} mutants of any age, TUNEL-positive cells were never seen. Thus, loss of *da* function reduces normally occurring apoptosis of germline cysts at the region 2a/2b boundary.

Genetic interactions between *da* and signal transduction pathways

Since many aspects of the *da* mutant phenotype detailed here have been described previously for mutants in several signal transduction pathways, we examined genetic interaction phenotypes to identify which specific pathway(s) include da^{+} function. This approach has already been used to identify a connection between *da* and the *Notch* (*N*) signaling pathway (Cummings and Cronmiller, 1994), and we extended this by showing similar interactions between *da* and *deltex (dx)*, *Suppressor of deltex* [*Su(dx)*], or *Suppressor of Hairless* [*Su(H)*] (Table 2). In addition to the *N* pathway, we also found interactions with another regulatory pathway that is similarly required for differentiation of specific somatic cell types, namely the Janus Kinase/Signal Transducer and Activator of Transcription (JAK/STAT) pathway (Baksa et al., 2002; McGregor et al., 2002). Females doubly heterozygous for mutations in *da* and either *hopscotch* (encoding the *Drosophila* JAK) or *Stat92E* showed *da*-like ovarian defects (Table 2, Fig. 6A-C). These genetic interactions are consistent with a role for *da* in differentiation, but they could also result if *da* helps regulate somatic proliferation.

We obtained additional support for *da* involvement in the control of cell proliferation from genetic interactions with mutants in the epidermal growth factor receptor (EGFR) pathway. Most mutants in this pathway exhibited simple

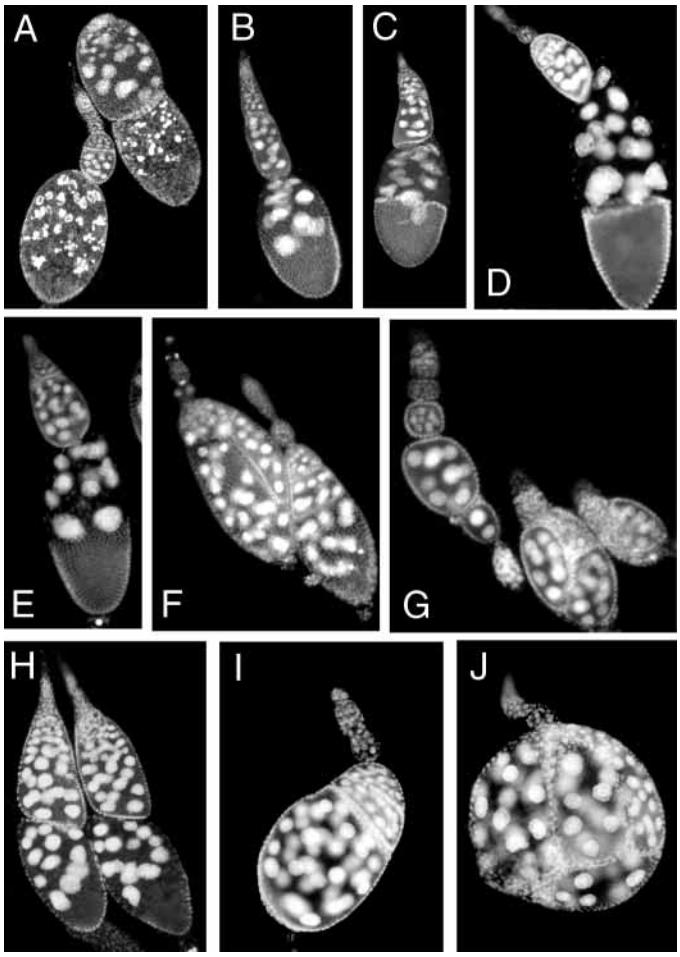

Fig. 6. Genetic interactions with mutants in the JAK/STAT and EGFR pathways. DAPI-stained ovarioles from flies doubly heterozygous for da^2 and: (A) hop^2, (B,C) $Stat92E^{1681}$, (D) grk^{HK36}, (E) sos^{e4G}, (F) phl^{c110}, and (G) rl^{Sem}. da^2 also acts as a dominant enhancer of top^{IP02}/top^1 (H) and $brn^{fs.107}/brn^{1.6P6}$ (I,J). The ovary interaction phenotypes are indistinguishable from those of *da* alone, except for the round ovariole morphology with *brn*.

Table 2. Genetic interactions between *da* and several signal transduction pathways result in follicle formation defects

Genotype	Frequency of ovarioles with follicular defects (number scored)
Notch pathway	
$Su(H)/da^2$	30% (308)
$dx^{S1M}/+$; $da^2/+$	58% (142)
$dx/+$; $da^2/+$	37% (363)*
$Su(dx)^2/da^2$	64% (324)
JAK/STAT pathway	
$hop^2/+$; $da^2/+$	26% (223)*
$da^2/+$; $Stat92E^{1681}/+$	78% (311)†
EGFR pathway	
grk^{HK36}/da^2	27% (249)
grk^{WG41}/da^2	15% (167)
spi^{A14}/da^2	51% (213)
spi^{OE92}/da^2	52% (331)
top^1/top^{IP02} da^2	93% (94)
top^{IP02} $da^2/+$	2% (61)
top^1/top^{IP02}	2% (53)
drk^{e0A}/da^2	58% (54)
sos^{e4G}/da^2	53% (93)
$da^2/+$; $Ras85D^{e1B}/+$	43% (79)
$phl^7/+$; $da^2/+$	71% (119)
$Dsor1^{S-1221}/+$; $da^2/+$	37% (86)
rl^{S-135}/da^2	41% (73)§
rl^{Sem}/da^2	73% (209)§
$da^2/+$; $pnt^{7825}/+$‡	55% (192)
aop^{IP}/da^2‡	0% (259)
aop^{IIS}/da^2‡	0% (371)
$brn^{1.6P6}/brn^{fs.107}$; $da^2/+$	53% (127)¶
$brn^{1.6P6}/brn^{fs.107}$; $CyO/+$	14% (140)¶
$brn^{fs.107}/brn^{fs.107}$; $da^2/+$	36% (47)¶
$brn^{fs.107}/brn^{fs.107}$; $CyO/+$	3% (31)¶
$sev^{d2}/+$; $da^2/+$††	0% (80)
$boss/da^2$††	0% (150)

Full gene names: *Suppressor of Hairless* [*Su(H)*], *deltex* (*dx*), *Suppressor of deltex* [*Su(dx)*], *hopscotch* (*hop*), *Signal-transducer and activator of transcription protein at 92E* (*Stat92E*), *gurken* (*grk*), *spitz* (*spi*), *torpedo* (*top*), *downstream of receptor kinase* (*drk*), *Son of sevenless* (*Sos*), *Ras oncogene at 85D* (*Ras85D*), *pole hole* (*phl*), *Downstream of raf1* (*Dsor1*), *rolled* (*rl*), *pointed* (*pnt*), *brainiac* (*brn*), *anterior open* (*aop*), *sevenless* (*sev*), *and bride of sevenless* (*boss*).

‡Targets of the EGFR pathway. ††From an independent receptor tyrosine kinase pathway. Ovaries from mated females at room temperature were examined 4-6 days after eclosion except as follows: §7-9 days after eclosion; *8-11 days after eclosion; †9 days after eclosion; ¶7 days at restrictive temperature (18°C).

second site noncomplementation with a *da* null allele (Table 2, Fig. 6D-G). One puzzling set of interactions involved the gene encoding MAP kinase. In combination with *da*, both loss-of-function and gain-of-function *rolled (rl)* alleles produced morphologically indistinguishable mutant ovaries, although the frequency of defects was higher with the gain-of-function allele (rl^{Sem}). This observation could mean that both EGFR pathway activation states are functional, albeit at different points in the cell cycle, as is the case in the eye (Baker and Yu, 2001). For *torpedo (top)* and *brainiac (brn)*, which did not show mutant phenotypes as double heterozygotes with da^2, *da* did act as a dominant enhancer of heteroallelic mutant genotypes in each case. All of the observed mutant phenotypes were morphologically indistinguishable from *da* loss-of-function phenotypes with the exception that those involving *top* and *brn* had additional defects not normally associated with *da* (Fig. 6H-J). The *da-top* mutant ovarioles had occasional discontinuities in the follicular epithelium (not shown) similar to those previously reported for *top* (Goode et al., 1992); however, this *top*-specific defect was not enhanced by *da*. In the *da-brn* mutant ovaries, while most ovarioles were simply *da*-like, occasional ovarioles consisted of large compartmentalized spheres attached to germaria. The compartments within these structures appeared to be delineated by follicular epithelium that separated groups of germline cells.

Finally, we tested the *hedgehog (hh)* pathway for involvement with *da*, since this pathway has been shown to regulate somatic cell proliferation by acting as a stem cell factor. By conferring stem cell properties on multiple somatic cells, ectopic overexpression of *hh* leads to overproduction of somatic cells, resulting in long interfollicular stalks (Forbes et al., 1996a; Zhang and Kalderon, 2001). We found that da^+ was required for *hh*-induced somatic cell overproliferation. The phenotype produced by induced ectopic *hh* expression was partially suppressed when females were also heterozygous for a *da* null allele: interfollicular cell populations were notably

smaller (compare Fig. 7A with 7B,C). Moreover, the complete elimination of *da* from the somatic ovary was epistatic to induced *hh*: the phenotype was indistinguishable from the *da* null phenotype alone (Fig. 7D). Apparently, the extra somatic stem cells induced by ectopic *hh*, or their own mitotic derivatives, required da^+ to proliferate. Conversely, elevated da^+ levels enhanced the *hh*-induced increase in interfollicular cells (Fig. 7E,F). In addition to causing surplus cells, the increased da^+ dose also affected the behavior of those cells, resulting in the formation of branched stalks (Fig. 7F-H). Each stalk branch usually terminated with an apparently normal follicle, producing a novel 'lollipop' structure (Fig. 7F-H). Presumably, formation of 'lollipops' arose by interfollicular cell rearrangements, which only occurred after some critical mass of supernumerary cells was attained, since 'lollipops' were observed only in the vitellarium at some distance from the germarium. Thus, elevated *da* conferred behavioral changes to the excess interfollicular somatic cells, causing them to carry out the convergence and extension process that is characteristic of normal stalk cells (Godt and Laski, 1995).

DISCUSSION

We have shown that *da* has at least three distinct roles during ovarian follicle formation. First, *da* is an essential regulator of the proliferation of somatic cells. Second, *da* is required for the complete differentiation of interfollicular stalk cells. Third, *da* is the first identified genetic regulator of a checkpoint for cyst progression in region 2b of the germarium.

An expanded model for follicle formation

Integrating this information about *da* activities with several published models of early oogenesis leads to the following outline for the sequential steps required for the iterative production of follicles (Fig. 8). (1) Signaling by Hh protein from the terminal filament creates a somatic stem cell niche at the region 2a/2b boundary (Zhang and Kalderon, 2001). (2) Somatic stem cells produce undifferentiated mesenchymal cells that surround the germline cyst and compress it into the characteristic lens shape (King, 1970). (3) EGFR-mediated signaling from the germline cyst provides a continuous proliferative signal to somatic cells (Goode et al., 1996; Goode et al., 1992). (4) A second germline-to-soma signal, Dl, induces the somatic cells, located between adjacent cysts in region 2b/3, to begin differentiating as polar cells (Lopez-Schier and St. Johnston, 2001). (5) Other somatic cells, which contact only a single germline cyst, differentiate as cuboidal epithelial cells. (6) The differentiating polar cells signal to neighboring cells to refine polar cell number, recruit stalk cells and promote local somatic cell proliferation. (7) The stalk cells migrate between the polar cells associated with each cyst and converge and extend to form a single column of cells as they terminally differentiate. In this scheme, *da* function appears to contribute to steps 2, 3, 6 and 7.

The initial requirement for *da* during follicle formation is somatic cell proliferation during steps 2 and 3. The straightforward observation that one extra copy of da^+ results in excess somatic cell production, while *da* loss of function leads to an insufficient number of somatic cells for germline cyst envelopment, demonstrates a role for *da* in proliferation. The genetic interactions between *da* and every component of the EGFR pathway, which is also known to regulate somatic proliferation through mid-oogenesis, suggest that *da* and the EGFR pathway cooperate to control cell division. Gurken has been identified as the germline-localized ligand for this proliferative function (Goode et al., 1996; Neuman-Silberberg and Schüpbach, 1996); however, *grk* null ovaries have a relatively low frequency of follicle formation defects (Goode et al., 1996) (our unpublished data). The genetic interaction that we observed between *da* and *spi* implicates Spi as a second ligand for EGFR in proliferation, although this must be a somatic signal, since *spi* expression is restricted to somatic cells (Wasserman and Freeman, 1998). Finally, although there is no evidence for *da* acting during specification of the somatic stem cells (step 1), it may control their proliferation once founded. Alternatively, *da* control of proliferation may be limited to the progeny of the stem cells. Either possibility is consistent with suppression of the ectopic *hh* phenotype in *da* heterozygotes and the complete epistasis of da^{lyh}.

Although *da*'s role in the control of somatic proliferation is unknown, it probably involves regulation of cell cycle progression. Connections between EGFR signaling and cell cycle progression have already been established in the R2-R5 photoreceptor cells in the morphogenetic furrow of the eye, where EGFR signal transduction is required for G_2/M progression, but signal inactivity is necessary for G_1/S progression (Baker and Yu, 2001). Coincidentally, Da protein levels are high in those cells, and *da* function is required for their G_1/S progression (Brown et al., 1996). A similar connection between *da* and cell cycle control in the ovary is implicated by our observation that *da* exhibits genetic interaction phenotypes with both loss of function (rl^-) and persistently activated (rl^{Sem}) MAPK alleles. Loss of EGFR signaling would be expected to delay cell cycle progression at the G_2/M transition, but persistent $MAPK^{Sem}$ activity, being a poor substrate for the inactivating phosphatase (Karim and Rubin, 1999), would delay the cell cycle at the G_1/S transition. In either situation additionally reducing the *da* dose, which itself would slow G_1/S progression, would lead to the mutant phenotype we observed in genetic interactions, and the higher frequency of defects with rl^{Sem} is consistent with both *da* and rl^{Sem} impacting on the same stage of the cell cycle.

There is probably no role for *da* in induction of polar cells or the differentiation of follicular epithelium (steps 4 and 5). It is clear from clonal analysis that both *N* and *fringe (fng)* are required in the soma for induction of polar cells in response to Dl signaling from the germline (Grammont and Irvine, 2001; Lopez-Schier and St. Johnston, 2001). The *N* response is localized to a thin stripe of cells in region 2b of the germarium (Jordan et al., 2000). This single layer of cells will eventually give rise to two sets of polar cells, one for the anterior pole of the older adjacent cyst and one for the posterior pole of the younger adjacent cyst. Because these cells are sandwiched between two germline cysts, their exposure to Dl should be higher (assuming uniform distribution of the protein) than the exposure to neighboring cells that contact only a single germline cyst. Thus, *N*-mediated polar cell induction occurs only between two germline cysts, where Dl signaling is highest. Since *fng* expression is also high in these cells, it is likely that *fng* sensitizes N to respond to Dl, as it does in

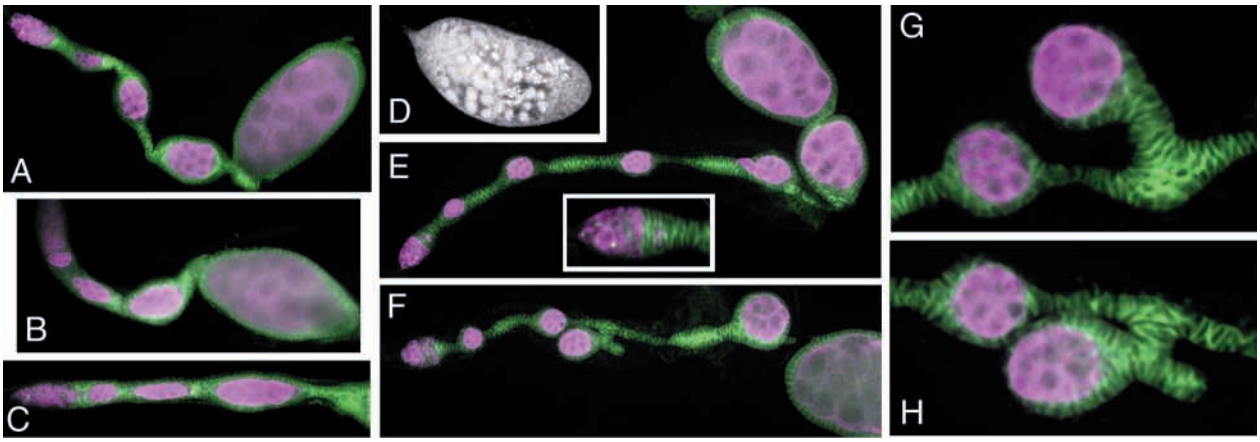

Fig. 7. Genetic interactions with ectopic *hh*. (A) Ectopic expression of *hh* produces excess somatic cells and long stalks. (B,C) Ectopic *hh* phenotype is partially suppressed in a da^{2} heterozygous genotype; follicles are often compressed into an elongated shape (C). (D) The *da* mutant genotype (da^{lyh}/da^{2}) is completely epistatic to ectopic *hh*. (E-H) Elevated da^{+} (*DpB231;* da^{lyh}) enhances the ectopic *hh* phenotype: (E) interfollicular cell number is increased (inset: loss of region 3 cyst characteristic of excess da^{+}). (F) Frequent branched stalks usually terminate with otherwise detached follicles to form 'lollipop-like' structures. (G,H) Enlarged view of 'lollipops'. Staining: Hts (green), Vasa (magenta), DAPI (grayscale).

imaginal discs (Grammont and Irvine, 2001; Jordan et al., 2000). In the absence of sufficiently high Dl levels, cells in contact with the germline contribute to the overlying epithelium of that cyst. No specific genes have been identified that affect the morphological differentiation of the follicular epithelium; however, *N* mutant clones in the epithelium fail to lose FasIII expression after entering the vitellarium and fail to switch from a mitotic cycle to an endocycle at stage 6, indicating that later aspects of differentiation of these epithelial cells are dependent upon low levels of *Dl* germline signaling (Deng et al., 2001; Lopez-Schier and St. Johnston, 2001). Initially, however, for undifferentiated mesenchymal cells to become epithelial, a different germline-to-soma signal may be involved. Alternatively, these cells may only require polarizing contact with the germline, mediated by cell adhesion molecules.

Complete polar cell differentiation (step 6) depends on *da* and is required for several non autonomous polar cell functions. The first function of differentiating polar cells is stalk cell recruitment. Clonal analysis of *fng* and *N* has shown that the function of these genes is required in the polar cells to form interfollicular stalks (Grammont and Irvine, 2001; Lopez-Schier and St. Johnston, 2001). In fng^{-} clones in which no distinct stalk is visible, the stalk-specific enhancer trap *B1-93F* is expressed in a peripheral cluster of cells at the junction between two incompletely separated follicles (Grammont and Irvine, 2001); we observed the same clusters in N^{ts1} mutant ovaries (data not shown). This arrangement would result if the

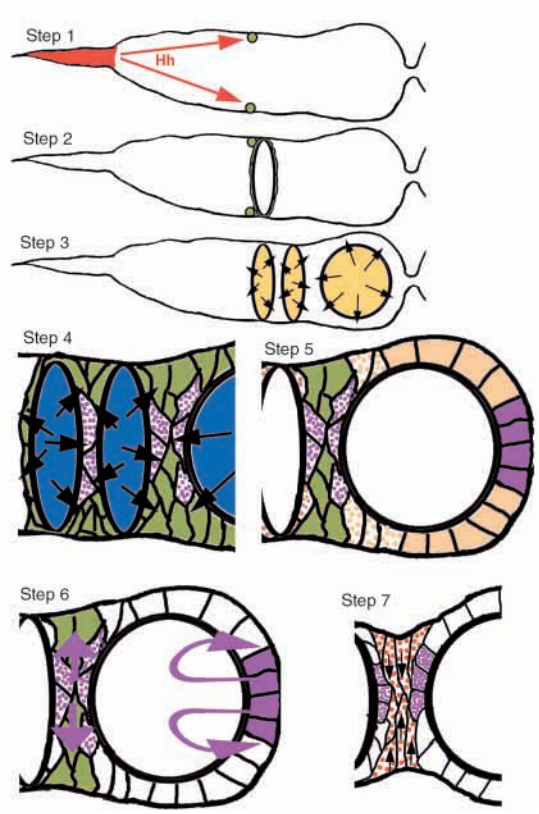

Fig. 8. An expanded model for follicle formation. Step 1: signaling by *hh* from the terminal filament (red) creates a somatic stem cell niche at the region 2a/2b boundary, conferring stem cell characteristics on 2 somatic cells (green). Step 2: somatic stem cells produce undifferentiated mesenchymal cells (green) that surround the germline cyst and compress it into a lens shape in region 2b Step 3: EGFR signaling from the germline (yellow) provides a continuous proliferation signal to somatic cells. Step 4: Dl signaling (blue) induces somatic cells between adjacent cysts in region 2b to initiate polar cell differentiation (purple stippling). Step 5: Somatic cells that physically contact only one germline cyst differentiate as cuboidal epithelial cells (beige). Step 6: differentiating polar cells provide a 'booster' proliferative signal, while recruiting remaining somatic cells in region 2b to form stalks (straight purple arrows); these could be distinct signals. In region 3 lateral inhibition (curved purple arrows) eventually refines the polar cell number to two. Step 7: differentiating stalk cells (orange stippling) converge and extend (arrows) between polar cells of adjacent cysts to form an interfollicular stalk. Steps 2, 3, 6 and 7 require discrete da^{+} functions.

differentiating polar cells normally recruit stalk cells from the periphery, where a population of undifferentiated somatic cells is not in contact with any germline cyst. Like *N* and *fng*, *da* interferes with recruitment of stalk cells from the periphery, since similar 'stalk cell' clusters were often observed in hypomorphic mutant ovarioles. In *da* mutant ovaries with more extreme defects, the 'stalk cells' were actually integrated within the follicular epithelium, suggesting that there were insufficient somatic cells to complete the epithelium. Thus, when there are sufficient somatic epthelial cells to cover the germline cyst completely (weak da^- phenotype), differentiating stalk cells never touch the germline; however, when there are not enough somatic cells (strong da^- phenotype), differentiating stalk cells consequently make contact with the germline and become incorporated into the epithelium. We propose that a second function of differentiating polar cells is the production of a 'booster' proliferative signal to ensure sufficient somatic cells to form a stalk. A number of genetic manipulations [elevated *da*; ectopic N^{intra}, *Dl*, *unpaired* (*upd*) or *hh*; and clones of *patched*$^-$ or of double mutant *Protein kinaseA*$^-$ (*PKA/Pka-C1*) *Suppressor of fused*$^-$ (*Su(fu)*)] lead to overproduction of somatic cells within the germarium, and in every case the result is excess interfollicular cells (Forbes et al., 1996a; Forbes et al., 1996b; Larkin et al., 1996; Larkin et al., 1999; McGregor et al., 2002; Zhang and Kalderon, 2000). (To what extent these interfollicular cells organize into recognizable stalks likely reflects each genotype's impact on stalk cell differentiation.) These phenotypes implicate all of these genes in proliferation control: the *N* pathway (*N*, *Dl*), the JAK/STAT pathway (*upd*), and the *hh* pathway (*hh, ptc*, *PKA, Su(fu)*). A proliferative role for the *N* pathway is substantiated by reconsideration of the loss-of-function phenotypes (N^{ts1}, *fng*), in which 'stalk cells' are observed within the follicular epithelium (Grammont and Irvine, 2001) (our unpublished data); the *N* pathway may be generally required for somatic proliferation, like *da*. However, for the JAK/STAT pathway, whose only known ligand is encoded by *upd* (Harrison et al., 1998), expression of the ligand is restricted to the polar cells in the ovary (McGregor et al., 2002). Although other studies have demonstrated roles for the JAK/STAT pathway that are limited to polar and stalk cell specification and/or differentiation during follicle formation (Baksa et al., 2002; McGregor et al., 2002), the effects of ectopic *upd*, together with the genetic interaction phenotypes between *da* and JAK/STAT pathway mutants, suggest that JAK/STAT is also a regulator of proliferation in the ovary, as it is elsewhere (Dearolf, 1999). If so, this would require expression of *upd* in region 2b, earlier than previously detected (Silver and Montell, 2001; McGregor et al., 2002). Finally, complete polar cell differentiation includes refinement to two polar cells; a number of markers [FasIII (Ruohola et al., 1991), *A101* (Johnson et al., 1995), *fng* (Jordan et al., 2000), *PZ80* (McGregor et al., 2002)] show that variable numbers (4-8 between adjacent germline cysts) of polar cells form but always refine to 2 per pole by the time a follicle matures to stage 4. In a number of mutants, including *da*, excess polar cells often persist past stage 4 (McGregor et al., 2002; Johnson et al., 1995; Ruohola et al., 1991), suggesting a failure in refinement.

The differentiation of stalk cells (step 7) also requires *da*. In weak da^- phenotypes where cells expressing stalk cell markers were seen in clusters physically isolated from the germline cyst by an epithelial layer, the 'stalk cells' did not converge and extend to form a stalk, as wild-type stalk cells would. This failure to form stalks could result from defects in recruitment of stalk cells by polar cells (step 6), in stalk cell differentiation, or both. Consistent with a proactive role for *da* in stalk cell differentiation, genotypes with elevated *da* levels occasionally formed stalk-like structures at the expense of the follicular epithelium. Indeed, Da protein levels normally remain high in the stalk and polar cells, even after they have dropped in the follicular epithelium (Cummings and Cronmiller, 1994). Additionally, stalk-like differentiation of the excess somatic cells generated by ectopic *hh* was *da*-dependent: reduced *da* resulted in more aggregation (i.e. less convergence and extension) and increased *da* resulted in more convergence and extension (i.e. less aggregation). In this context, the 'lollipop' phenotype reflects the acquisition of a stalk-like characteristic by excess somatic cells; *hh*-induced somatic cells that rearrange in the vitellarium to form cables running along the sides of follicles, as shown by Forbes et al. (Forbes et al., 1996a), converge and extend to form a 'lollipop', when *da* is increased. Relatively high Da levels appear to be required to drive convergence and extension in differentiating stalk cells. This *da* requirement may involve transcriptional activation of stalk-specific genes, since the expression of two stalk cell markers is reduced in strong da^- phenotypes. However, reduced marker expression could result indirectly from incorporation of 'stalk cells' into the follicular epithelium, where stalk-specific gene expression may be repressed.

A checkpoint for germline cyst progression

Successful follicle formation requires the right balance of somatic cells per germline cyst, such that ratios that are too low activate germline apoptosis to abort cyst progression in the germarium; the function of this cyst progression checkpoint was first demonstrated in nutrient-deprived flies (Drummond-Barbosa and Spradling, 2001). The mechanism for assessing the soma-to-germline ratio is completely unknown; however, the relative balance of cells is evaluated as each 16-cell cyst enters region 2b of the germarium. Thus, environmental variables such as nutrition could lead to activation of the cyst progression checkpoint either by increasing germline cyst production or retarding somatic cell production. If these two cell populations (germline and soma) have different nutritional requirements, cyst apoptosis might be activated only at nutritional extremes: at one extreme (low nutritional values), slackened somatic cell proliferation does not keep pace with normal cyst production, resulting in aborted cyst progression, while at the other extreme (high nutritional values), accelerated cyst production outpaces normal somatic cell proliferation, resulting in a similar termination of cyst progression. Only in situations in which the rates of cyst production and somatic cell proliferation are balanced (e.g., intermediate nutritional values) would activation of the cyst progression checkpoint be unnecessary. Age could affect the proliferation rate of either of these two cell populations, and we have observed that the frequency of cyst apoptosis in the germarium does increase with age. Other environmental conditions that have been shown to affect egg production, such as temperature, humidity, prior anesthesia, adult crowding, mate abundance and dessication state (reviewed by King, 1970; Ashburner, 1989), should be examined similarly for effects on cyst progression. Checkpoint

activation is also influenced by the genetic background as the frequency of apoptosis varied among wild-type strains. How a somatic cell deficit, once detected, leads to activation of apoptosis in the germline cyst is unknown; however, our evidence indicates that somatic cells are involved in the process.

Numerous observations from our analyses of *da* mutant phenotypes identify *da* as a key component in the soma's regulation of the cyst progression checkpoint. The significant reduction in cyst degradation (as viewed either by Acridine Orange staining or TUNEL) in *da* loss-of-function mutants indicates that the checkpoint is *da*-dependent, and since Da protein is absent from the germline (Cummings and Cronmiller, 1994), it is the gene's somatic dose that is critical in this process. This is consistent with the phenotype caused by moderate elevations of *da* (by chromosomal duplications) in which the checkpoint appears to function normally; the increased somatic cell production provided by the weaker duplication only resulted in longer interfollicular stalks, while the stronger duplication additionally resulted in more cysts surviving the checkpoint and being packaged into follicles due to the further increased production of somatic cells. Additional evidence that *da* normally contributes to the checkpoint comes from the analysis of the effects of higher elevations of *da*, which can lead to ectopic cyst degradation in the germarium. The synergistic interaction between the *da* dose and an environmental variable (i.e. cyst degradation in flies with elevated *da* levels increased with age) suggests that environmental conditions can sensitize the checkpoint to activation by *da*. Moreover, the apoptotic checkpoint is only activated in post-mitotic cysts, since elevated *da* did not lead to the degradation of still-dividing cysts, even when these slipped into region 2b or 3 of the germarium. Although only post-mitotic cysts appear capable of activating the apoptosis pathway, cells in the adjacent soma are responsible for monitoring the germline cyst/somatic cell balance and sending an activating signal. The role of *da* in those cells could entail either positive or negative regulation. For positive regulation, da^+ would promote the generation of a proapoptotic factor as an integral part of the checkpoint. For negative regulation, da^+ would repress an antiapoptotic (i.e. prosurvival) factor; such a factor would normally be required for the maintenance of post-mitotic cysts in the germarium. The identification of additional genetic components of the checkpoint will help distinguish between these two models.

We are especially grateful to Stacey Sedore for performing the TUNEL reactions. We thank Jay Hirsh, Michele Lamka Emily Ozdowski, and Stacey Sedore for helpful comments on the manuscript and C. Dearolf and D. Harrison for providing manuscripts prior to publication. J. E. S. was supported by an NIGMS training grant (5T32 GM08136). This work was supported by a grant from the National Science Foundation to C. C.

REFERENCES

Abrams, J. M., White, K., Fessler, L. I. and Steller, H. (1993). Programmed cell death during *Drosophila* embryogenesis. *Development* **117**, 1-15.

Ashburner, M. (1989). *Drosophila*: *A Laboratory Handbook.* Cold Spring Harbor, NY: Cold Spring Harbor Laboratory Press.

Baker, N. E. and Yu, S. Y. (2001). The EGF receptor defines domains of cell cycle progression and survival to regulate cell number in the developing *Drosophila* eye. *Cell* **104**, 699-708.

Baksa, K., Parke, T., Dobens, L. L. and Dearolf, C. R. (2002). The Drosophila STAT protein, Stat92E, regulates follicle cell differentiation during oogenesis. *Dev. Biol.* **243**, 166-175.

Barrett, K. L., Willingham, J. M., Garvin, A. J. and Willingham, M. C. (2001). Advances in cytochemical methods for detection of apoptosis. *J. Histochem. Cytochem.* **49**, 821-832.

Brown, N. L., Paddock, S. W., Sattler, C. A., Cronmiller, C., Thomas, B. J. and Carroll, S. B. (1996). *daughterless* is required for *Drosophila* photoreceptor cell determination, eye morphogenesis, and cell cycle progression. *Dev. Biol.* **179**, 65-78.

Cabrera, C. V. and Alonso, M. C. (1991). Transcriptional activation by heterodimers of the *achaete-scute* and *daughterless* gene products of *Drosophila*. *EMBO J.* **10**, 2965-2973.

Caudy, M., Grell, E. H., Dambly-Chaudiere, C., Ghysen, A., Jan, L. Y. and Jan, Y. N. (1988). The maternal sex determination gene *daughterless* has zygotic activity necessary for the formation of peripheral neurons in Drosophila. *Genes Dev.* **2**, 843-852.

Cummings, C. A. and Cronmiller, C. (1994). The *daughterless* gene functions together with *Notch* and *Delta* in the control of ovarian follicle development in *Drosophila*. *Development* **120**, 381-394.

de Cuevas, M. and Spradling, A. C. (1998). Morphogenesis of the *Drosophila* fusome and its implications for oocyte specification. *Development* **125**, 2781-2789.

Dearolf, C. R. (1999). JAKs and STATs in invertebrate model organisms. *Cell Mol. Life Sci.* **55**, 1578-1584.

Deng, W. M., Althauser, C. and Ruohola-Baker, H. (2001). Notch-Delta signaling induces a transition from mitotic cell cycle to endocycle in *Drosophila* follicle cells. *Development* **128**, 4737-4746.

Deshpande, G., Stukey, J. and Schedl, P. (1995). *scute (sis-b)* function in *Drosophila* sex determination. *Mol. Cell. Biol.* **15**, 4430-4440.

Drummond-Barbosa, D. and Spradling, A. C. (2001). Stem cells and their progeny respond to nutritional changes during *Drosophila* oogenesis. *Dev. Biol.* **231**, 265-278.

FlyBase (2002). The FlyBase database of the *Drosophila* genome projects and community literature. *Nucleic Acids Res.* **30**, 106-108.

Forbes, A. J., Lin, H., Ingham, P. W. and Spradling, A. C. (1996a). *hedgehog* is required for the proliferation and specification of ovarian somatic cells prior to egg chamber formation in *Drosophila*. *Development* **122**, 1125-1135.

Forbes, A. J., Spradling, A. C., Ingham, P. W. and Lin, H. (1996b). The role of segment polarity genes during early oogenesis in *Drosophila*. *Development* **122**, 3283-3294.

Godt, D. and Laski, F. A. (1995). Mechanisms of cell rearrangement and cell recruitment in *Drosophila* ovary morphogenesis and the requirement of *bric a brac*. *Development* **121**, 173-187.

Gold, R., Schmied, M., Giegerich, G., Breitschopf, H., Hartung, H. P., Toyka, K. V. and Lassmann, H. (1994). Differentiation between cellular apoptosis and necrosis by the combined use of *in situ* tailing and nick translation techniques. *Lab. Invest.* **71**, 219-225.

Gonzalez-Crespo, S. and Levine, M. (1993). Interactions between dorsal and helix-loop-helix proteins initiate the differentiation of the embryonic mesoderm and neuroectoderm in *Drosophila*. *Genes Dev.* **7**, 1703-1713.

Goode, S., Morgan, M., Liang, Y. P. and Mahowald, A. P. (1996). *Brainiac* encodes a novel, putative secreted protein that cooperates with Grk TGF alpha in the genesis of the follicular epithelium. *Dev. Biol.* **178**, 35-50.

Goode, S., Wright, D. and Mahowald, A. P. (1992). The neurogenic locus *brainiac* cooperates with the *Drosophila* EGF receptor to establish the ovarian follicle and to determine its dorsal- ventral polarity. *Development* **116**, 177-192.

Grammont, M. and Irvine, K. D. (2001). *fringe* and *Notch* specify polar cell fate during *Drosophila* oogenesis. *Development* **128**, 2243-2253.

Harrison, D. A., McCoon, P. E., Binari, R., Gilman, M. and Perrimon, N. (1998). *Drosophila unpaired* encodes a secreted protein that activates the JAK signaling pathway. *Genes Dev.* **12**, 3252-3263.

Hassan, B. and Vaessin, H. (1997). Daughterless is required for the expression of cell cycle genes in peripheral nervous system precursors of *Drosophila* embryos. *Dev. Genet.* **21**, 117-122.

Jarman, A. P., Brand, M., Jan, L. Y. and Jan, Y. N. (1993). The regulation and function of the helix-loop-helix gene, *asense*, in *Drosophila* neural precursors. *Development* **119**, 19-29.

Johnson, E., Wayne, S. and Nagoshi, R. (1995). *fs(1)Yb* is required for ovary follicle cell differentiation in *Drosophila melanogaster* and has genetic

interactions with the *Notch* group of neurogenic genes. *Genetics* **140**, 207-217.

Jordan, K. C., Clegg, N. J., Blasi, J. A., Morimoto, A. M., Sen, J., Stein, D., McNeill, H., Deng, W. M., Tworoger, M. and Ruohola-Baker, H. (2000). The homeobox gene *mirror* links EGF signalling to embryonic dorso-ventral axis formation through Notch activation. *Nat. Genet.* **24**, 429-433.

Karim, F. D. and Rubin, G. M. (1999). PTP-ER, a novel tyrosine phosphatase, functions downstream of Ras1 to downregulate MAP kinase during *Drosophila* eye development. *Mol. Cell* **3**, 741-750.

Keyes, L. N., Cline, T. W. and Schedl, P. (1992). The primary sex determination signal of *Drosophila* acts at the level of transcription. *Cell* **68**, 933-943.

King, R. C. (1970). *Ovarian Development in* Drosophila melanogaster. New York: Academic Press.

King-Jones, K., Korge, G. and Lehmann, M. (1999). The helix-loop-helix proteins dAP-4 and daughterless bind both in vitro and in vivo to SEBP3 sites required for transcriptional activation of the *Drosophila* gene Sgs-4. *J. Mol. Biol.* **291**, 71-82.

Larkin, M. K., Deng, W., Holder, K., Tworoger, M., Clegg, N. and Ruohola-Baker, H. (1999). Role of Notch pathway in terminal follicle cell differentiation during *Drosophila* oogenesis. *Dev. Genes Evol.* **209**, 301-311.

Larkin, M. K., Holder, K., Yost, C., Giniger, E. and Ruohola-Baker, H. (1996). Expression of constitutively active *Notch* arrests follicle cells at a precursor stage during *Drosophila* oogenesis and disrupts the anterior-posterior axis of the oocyte. *Development* **122**, 3639-3650.

Lopez-Schier, H. and St. Johnston, D. (2001). *Delta* signaling from the germ line controls the proliferation and differentiation of the somatic follicle cells during *Drosophila* oogenesis. *Genes Dev.* **15**, 1393-1405.

McGregor, J. R., Xi, R. and Harrison, D. A. (2002). JAK signaling is somatically required for follicle cell differentiation in *Drosophila*. *Development* **129**, 705-717.

Misquitta, L. and Paterson, B. M. (1999). Targeted disruption of gene function in *Drosophila* by RNA interference (RNA-i): A role for *nautilus* in embryonic somatic muscle formation. *Proc. Natl. Acad. Sci. USA* **96**, 1451-1456.

Mpoke, S. S. and Wolfe, J. (1997). Differential staining of apoptotic nuclei in living cells: application to macronuclear elimination in *Tetrahymena*. *J. Histochem. Cytochem.* **45**, 675-683.

Murre, C., Bain, G., van Dijk, M. A., Engel, I., Furnari, B. A., Massari, M. E., Matthews, J. R., Quong, M. W., Rivera, R. R. and Stuiver, M. H. (1994). Structure and function of helix-loop-helix proteins. *Biochim. Biophys. Acta* **1218**, 129-135.

Neuman-Silberberg, F. S. and Schüpbach, T. (1996). The Drosophila TGF-alpha-like protein Gurken: expression and cellular localization during *Drosophila* oogenesis. *Mech. Dev.* **59**, 105-113.

Pagliuca, A., Gallo, P., de Luca, P. and Lania, L. (2000). Class A helix-loop-helix proteins are positive regulators of several cyclin-dependent kinase inhibitors' promoter activity and negatively affect cell growth. *Cancer Res.* **60**, 1376-1382.

Patel, N. H., Snow, P. M. and Goodman, C. S. (1987). Characterization and cloning of *fasciclin III*: a glycoprotein expressed on a subset of neurons and axon pathways in *Drosophila*. *Cell* **48**, 975-988.

Peverali, F. A., Ramqvist, T., Saffrich, R., Pepperkok, R., Barone, M. V. and Philipson, L. (1994). Regulation of G_1 progression by E2A and Id helix-loop-helix proteins. *EMBO J.* **13**, 4291-4301.

Ruohola, H., Bremer, K. A., Baker, D., Swedlow, J. R., Jan, L. Y. and Jan, Y. N. (1991). Role of neurogenic genes in establishment of follicle cell fate and oocyte polarity during oogenesis in *Drosophila*. *Cell* **66**, 433-449.

Silver, D. L. and Montell, D. J. (2001). Paracrine signaling through the JAK/STAT pathway activates invasive behavior of ovarian epithelial cells in Drosophila. *Cell* **107**, 831-841.

Smith, J. E. and Cronmiller, C. (2001). The *Drosophila daughterless* gene autoregulates and is controlled by both positive and negative *cis* regulation. *Development* **128**, 4705-4714.

Spradling, A., Drummond-Barbosa, D. and Kai, T. (2001). Stem cells find their niche. *Nature* **414**, 98-104.

Styhler, S., Nakamura, A., Swan, A., Suter, B. and Lasko, P. (1998). *vasa* is required for GURKEN accumulation in the oocyte, and is involved in oocyte differentiation and germline cyst development. *Development* **125**, 1569-1578.

Wallace, K., Liu, T. H. and Vaessin, H. (2000). The pan-neural bHLH proteins DEADPAN and ASENSE regulate mitotic activity and cdk inhibitor *dacapo* expression in the *Drosophila* larval optic lobes. *Genesis* **26**, 77-85.

Wasserman, J. D. and Freeman, M. (1998). An autoregulatory cascade of EGF receptor signaling patterns the *Drosophila* egg. *Cell* **95**, 355-364.

Wei, Q., Marchler, G., Edington, K., Karsch-Mizrachi, I. and Paterson, B. M. (2000). RNA interference demonstrates a role for *nautilus* in the myogenic conversion of Schneider cells by *daughterless*. *Dev. Biol.* **228**, 239-255.

Xie, T. and Spradling, A. (2000). A niche maintaining germ line stem cells in the *Drosophila* ovary. *Nature* **290**, 328-330.

Yang, D., Lu, H., Hong, Y., Jinks, T. M., Estes, P. A. and Erickson, J. W. (2001). Interpretation of X chromosome dose at *Sex-lethal* requires non-E-box sites for the basic helix-loop-helix proteins SISB and Daughterless. *Mol. Cell. Biol.* **21**, 1581-1592.

Zaccai, M. and Lipshitz, H. D. (1996). Differential distributions of two adducin-like protein isoforms in the *Drosophila* ovary and early embryo. *Zygote* **4**, 159-166.

Zhang, Y. and Kalderon, D. (2000). Regulation of cell proliferation and patterning in *Drosophila* oogenesis by Hedgehog signaling. *Development* **127**, 2165-2176.

Zhang, Y. and Kalderon, D. (2001). Hedgehog acts as a somatic stem cell factor in the *Drosophila* ovary. *Nature* **410**, 599-604.

Zhao, F., Vilardi, A., Neely, R. J. and Choi, J. K. (2001). Promotion of cell cycle progression by basic helix-loop-helix E2A. *Mol. Cell. Biol.* **21**, 6346-6357.

Supplemental Table. Vital Acridine Orange staining of germaria

Genotype	Days after eclosion	% Acridine Orange-positive germaria	
		Overall	By female
Wild-type: OregonR	4-6	85.5 (*n*=269)	85.5±1.6 (*n*=10)
Wild-type: OregonR	2-4	59.4 (*n*=308)	59.2±2.6 (*n*=10)
Wild-type: CantonS	2-4	69.3 (*n*=381)	69.4±2.2 (*n*=10)
Wild-type: *white*^{1118}	4-6	61.9 (*n*=63)	61.9±2.6 (*n*=2)
Wild-type: *white*^{1118}	2-4	51.5 (*n*=297)	51.2±2.9 (*n*=10)
da^{7}/*da*^{s22}	2-4	4.2 (*n*=356)	4.1±1.2 (*n*=11)
da^{7}/*CyO* sisters	2-4	61.7 (*n*=334)	61.4±3.0 (*n*=10)
da^{lyh}/*da*^{lyh}	2-4	13.1 (*n*=252)	13.2±2.0 (*n*=10)
da^{lyh}/*CyO* sisters	2-4	82.4 (*n*=335)	82.1±3.3 (*n*=10)

FLY FOOD RECIPES

Yeast-agar-dextrose medium

(Source: Carpenter, J. M. (1950). A new semisynthetic food medium for Drosophila. *Dros. Inf. Serv.* **24**, 96-97.)
100 g Brewer's yeast
30 g Agar
200 g Dextrose
2 g K_2HPO_4
Mix dry ingredients and add:
1.6 l Water
50 ml Solution X (20 mg/ml $CaCl_2$)
50 ml Solution Y (20 mg/ml $FeSO_4{\cdot}7H_2O$)
50 ml Solution Z (16 g potassium sodium tartrate, 1 g NaCl, 1 g $MnCl_2{\cdot}4H_2O$ in 0.3 l)
Stir, autoclave for 5-25 minutes, allow to cool enough that when swirled will not boil over, and then add:
20 ml Tegosept solution (10% (w/v) methyl p-hydrobenzoate in 95% ethanol)
Pour vials.

Molasses-cornmeal-yeast medium

(Source: Applied Scientific, *Violet's Tasty Treats*)
1 l Molasses (unsulfured)
14 l Water
148 g Agar
1 l Corn meal
412 g Baker's yeast
225 ml Tegosept solution (10% (w/v) methyl p-hydrobenzoate in 95% ethanol)
80 ml Proprionic acid

Instructions for steam kettle

1. Add molasses and hot water to the kettle and turn on steam.
2. Measure and mix together the dry ingredients.
3. Turn on stirrer in the kettle, and add mixed dry ingredients.
4. Bring the mixture to a boil.
5. Turn down the steam halfway and boil for 10 minutes.
6. Turn off the steam and slowly add the Tegosept and proprionic acid.
7. Mix well and begin pouring vials.